

Received June 4, 2020, accepted June 28, 2020, date of publication July 2, 2020, date of current version July 14, 2020.

Digital Object Identifier 10.1109/ACCESS.2020.3006315

# Reset Strategy for Output Feedback Multiple Models MRAC Applied to DEAP

JAKUB BERNAT, (Member, IEEE), JAKUB KOŁOTA<sup>✉</sup>, AND DAMIAN CIEŚLAK

Faculty of Control, Robotics, and Electrical Engineering, Institute of Automatic Control and Robotics, Poznan University of Technology, 60-965 Poznan, Poland

Corresponding author: Jakub Bernat (jakub.bernat@put.poznan.pl)

This work was supported by the National Science Centre, Poland, through the SONATA 13 Project, under Grant 2017/26/D/ST7/00092.

**ABSTRACT** The smart actuators are rapidly developing in the recent years. Dielectric Electroactive Polymer actuators are very important smart actuators due to their features like softness, high force ratio, fast operation and silence. In recent year a set of dynamic models for DEAP actuators have been developed by various authors. Relying on these models it is possible to design an wide range of feedback controllers. In our work, we develop the indirect adaptive controller for Dielectric Electroactive Polymer actuator exploiting the multiple models approach with second layer adaptation. The results presented in this paper prove that in the case of piecewise continuous parameters, the benefits of second level adaptation can be lost. To solve this problem, a new resetting algorithm is proposed. The efficiency of the proposed control method is verified by a simulation on a simple motivation example and DEAP actuator model.

**INDEX TERMS** Adaptive control, smart materials, dielectric materials.

## I. INTRODUCTION

Smart materials are currently very perspective types of materials which actuate on different stimuli [1]. They are used to build smart actuators like Dielectric Electroactive Polymer (DEAP) actuators. Their main features like high force - volume ratio, soft membrane and fast response time made them useful to build many prototypes like pump [2], artificial muscles [3] and many others [4], [5]. A well designed control system is a very important aspect of design of these devices. To complete this task the nonlinear models of DEAP actuators were created [4], [6]–[9]. Relying on linear and nonlinear models a wide range of control systems for DEAP actuator was created. In works [7], [8], the PID controller was studied. The feedback control was designed to obtain high precision in work [10] and the compensation of hysteresis was proposed in work [11]. The sliding model control was used to build the controller in work [12]. The simple alternative was proposed in [13] where the open loop control is designed. Additionally, the machine learning approach is also studied. For instance, the reinforcement learning was used to find a neural network controller in work [14]. The intelligent control based on fuzzy system was designed in work [15].

The associate editor coordinating the review of this manuscript and approving it for publication was Engang Tian<sup>✉</sup>.

In our approach we study the design of an adaptive controller. This technique is well known for linear and nonlinear systems with linear parametrization [16]–[19]. In recent years, the multiple model technique was reported to improve significantly the transients of adaptive systems [18], [20], [21]. In the past, the multiple model technique based on switching strategy was applied to control system [18]. This technique is said to increase the efficiency of a controlled system, however, it required the oversized number of models [20]. This problem was solved in work [22] by applying an adaptive controller with second level adaptation. This solution was further studied for nonlinear system with linear parametrization [23], fractional system [24], observer design [25], [26] and artificial intelligence [27], [28]. The extension of this technique was also proposed in work [29] with second level adaptation based on error integration. A new approach presented in [30] considers a three layered adaptive control. The application of an adaptive control to linear varying systems and periodic systems is shown in [31] and [27] respectively.

In our work we design an adaptive controller for DEAP actuator taking into account an indirect adaptive control based on multiple models. It is worth mentioning that a direct adaptive controller was previously constructed by us in work [32]. In our work we exploit the recent technique called the second level adaptation. Our aim is to design a controller which operates for different working conditions. Therefore, the adaptive

control is applied to design the controller. We will show that the operation of an adaptive controller with a second level adaptation, the convergence of all multiple models occurs for a long time. In such conditions, the benefits of multiple models are very limited or lost. Therefore, a new algorithm based on resetting multiple models to initial structure is proposed. Therefore, the main contribution of this work is the introduction of the MRAC with multiple models and resetting algorithm. Firstly, a new algorithm is shortly described on a motivation example. Then it is applied to DEAP actuator.

The structure of this work is organized as follows. Section II describes the DEAP actuator model and its linearization. In Section III, the multiple model adaptation with resetting algorithm is introduced. Section IV shows the simulations of the presented schema for DEAP actuator. This section highlights the performance improvement caused by the resetting algorithm.

## II. DEAP ACTUATOR MODEL

In our work we consider Dielectric Electroactive Polymer (DEAP) actuator biased with mass [9], [32]. Taking into account our previous works [9], [32], the nonlinear model is given by:

$$\begin{aligned} \dot{x}_1 &= x_3 \\ \dot{x}_2 &= -\frac{k_e}{\eta_e}x_2 + \frac{k_e}{\eta_e}(\sqrt{s(x_1)} - 1) \\ \dot{x}_3 &= g - \frac{\bar{c}_1x_1}{ms(x_1)}\sigma_e(\sqrt{s(x_1)}, x_2) \\ &\quad - \frac{bx_1^2}{ml_0^3s(x_1)}x_3 + \frac{\bar{c}_1c_2}{m}x_1u^2 \\ y &= x_1 \end{aligned} \quad (1)$$

where  $x_1$  is the distance,  $x_2$  is the strain of the damper,  $x_3$  is the velocity and  $s(x_1) = 1 + \frac{x_1^2}{l_0^2}$ . The stress  $\sigma_e$  is defined as:

$$\begin{aligned} \sigma_e(\lambda_r, x_2) &= -k_e x_2 + k_e (\lambda_r - 1) + \underline{\sigma}_e(\lambda_r) \\ \underline{\sigma}_e(\lambda_r) &= \sum_{i=1}^3 [\beta_i \lambda_r^{\alpha_i} - \gamma_i \lambda_r^{-\alpha_i}] \\ \lambda_r &= \sqrt{s(x_1)} \end{aligned} \quad (2)$$

where  $\lambda_r$  is the stretch and fixed  $\alpha_i = 2, 4, 6$ . The actuator input  $u$  is the voltage and the output  $y$  is the distance. The DEAP actuator has an input nonlinearity  $u^2$ , which is simple to compensate by introducing a new input  $v = u^2$ . This approach was useful for instance in PID controller presented in work [33] for DEAP actuator. The presented model considers the mechanical stress of DEAP actuator and the electromechanical coupling. The mechanical stresses are described by viscoelastic and hyperelastic effect. The first is covered by two dampers represented by parameters  $k_e$ ,  $\eta_e$  and  $b$ . The hyperelastic stress is represented by  $\underline{\sigma}_e(\lambda_r)$ . The Maxwell stress combines an input voltage  $u$  with a mechanical part. The problem of DEAP actuator modeling is thoroughly discussed in works [1], [4], [6], [8], [10], [33]. The description of parameters are presented in Section IV along with their values.

In our work we consider an adaptive controller for DEAP actuator. The presented model does not have all state variables available for the measurement. It can be caused by the fact that, for instance, the strain of the damper  $x_2$  is virtual rather than physical signal. Further, the velocity in our work is also considered as not available. Therefore, we design an adaptive control from an output feedback. This makes the problem more challenging. In our approach we take into account Indirect Model Reference Controller, which is well known for linear systems. The nonlinear model (1) is linearized around the working point [32]. The nominal state and nominal voltage is found by solving equation:

$$\begin{aligned} 0 &= x_{3n} \\ 0 &= -\frac{k_e}{\eta_e}x_{2n} + \frac{k_e}{\eta_e}(\sqrt{s(x_{1n})} - 1) \\ 0 &= g - \frac{\bar{c}_1x_{1n}}{ms(x_{1n})}\sigma_e(\sqrt{s(x_{1n})}, x_{2n}) + \frac{\bar{c}_1c_2}{m}x_{1n}v_n \end{aligned} \quad (3)$$

This allows us to design a controller for a plant  $G_{DEAP}(s) = k_p \frac{Z_p(s)}{R_p(s)} = \frac{\Delta Y(s)}{\Delta V(s)}$ . The delta signals are calculated as  $\Delta y(t) = y(t) - y_n$  and  $\Delta v(t) = v(t) - v_n$ . The linearization of a nonlinear plant was used to obtain the coefficients of  $G_{DEAP}(s)$  [32]. During the simulations, it was found that coefficients of  $G_{DEAP}(s)$  vary for different working points. Therefore, the application of an adaptive control will allow to dynamically adjust to new parameter values.

## III. OUTPUT FEEDBACK MULTIPLE MODELS MRAC WITH RESETTING

The Indirect Model Reference Adaptive Controller is a well-known technique that allows for an adaptive output feedback control. In recent work, the crucial improvement of this technique was presented in recent work [20]. The application of multiple models with the second level adaptation allows for fast error convergence to 0. Furthermore, it requires less models than the switching techniques presented in [18]. In this section, we would like to introduce the resetting algorithm for the second level adaptive law in the case of piecewise constant parameters. Also we would like to show a short motivation example why such algorithm is required.

### A. MOTIVATION EXAMPLE

Let us consider the first order system:

$$\dot{x} = -ax + u \quad (4)$$

where  $a$  is the unknown but piecewise constant parameter,  $x$  is the state and  $u$  is the input. As in work [20], we construct identifiers (multiple models):

$$\dot{\hat{x}}_i = -a_m \hat{x}_i + (a_m - \hat{a}_i)x + u \quad (5)$$

with gradient adaptive law:

$$\dot{\hat{a}}_i = \gamma e_i x \quad (6)$$

where  $a_m > 0$  defines the identifier dynamics,  $\hat{x}_i$  is the estimated state,  $\hat{a}_i$  is the estimated parameter,  $\gamma$  is the adaptation gain,  $e_i = \hat{x}_i - x$  is the identification error and  $i = 1, 2$  because in the case of first order system with single

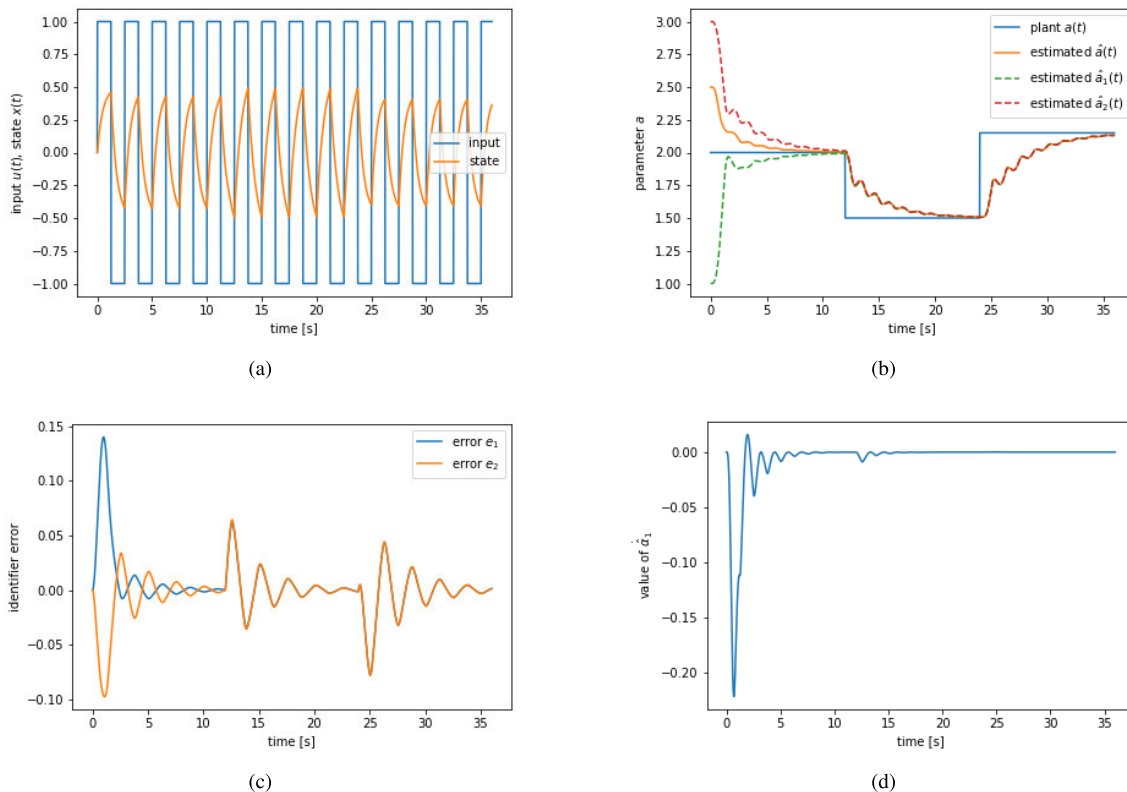


FIGURE 1. Simulation of first order system to present the influence of piecewise constant parameter  $a$  on multiple models algorithm.

unknown parameter only two virtual models are required. The estimated parameter is expressed as:

$$\begin{aligned} \hat{a} &= \hat{\alpha}_1 \hat{a}_1 + \hat{\alpha}_2 \hat{a}_2 \\ \hat{\alpha}_1 + \hat{\alpha}_2 &= 1 \end{aligned} \tag{7}$$

where  $\hat{a}_1, \hat{a}_2$  are the second layer weights. If the closed-loop control system was considered, the parameter  $\hat{a}$  would be used to calculate controller parameters. The second layer coefficient  $\hat{a}_1$  is estimated as:

$$\begin{aligned} \dot{\hat{\alpha}}_1 &= -\gamma_{mm} (e_1 - e_2) \epsilon \\ \epsilon &= \hat{\alpha}_1 e_1 + \hat{\alpha}_2 e_2 \\ \hat{\alpha}_2 &= 1 - \hat{\alpha}_1. \end{aligned} \tag{8}$$

where  $\gamma_{mm} > 0$  and  $\epsilon$  are the second level adaption gain and error respectively. In work [20], the stability of such systems was proved in the case of constant parameters. Further, it was shown that the second layer improves the transients of adaptive systems. We want to analyse a multiple models algorithm in the case of piecewise constant parameters as this analysis was not taken into consideration in the previous works for a multiple model adaptive control with a second layer. To simplify simulation, we consider open loop identification problem, which constitutes a part of IMRAC.

The simulation is performed for piecewise constant  $a$  (switch value in  $T_1 = 0[s], T_1 = 12[s]$  and  $T_3 = 24[s]$ ) and the squared wave input signal with amplitude 1 and period 2.5[s]. The initial values of estimated parameters are  $\hat{a}_1 = 1, \hat{a}_2 = 3, \hat{\alpha}_1 = 0.25, \hat{\alpha}_2 = 0.75$ . The identifiers coefficient  $a_m$

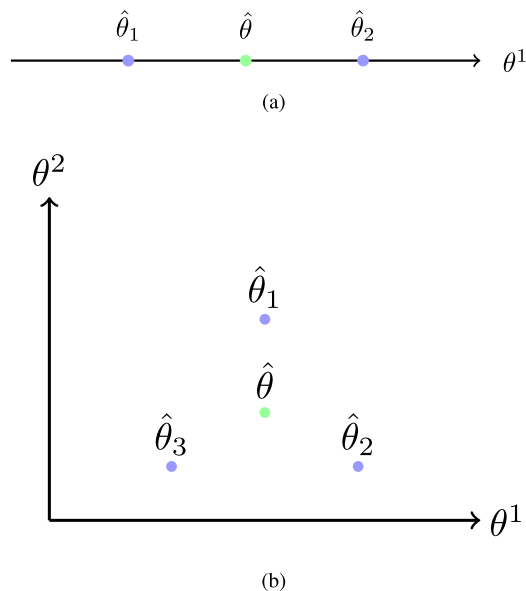


FIGURE 2. The estimated parameter  $\hat{\theta}$  and the structure of initial parameters  $\hat{\theta}_i$ ; (multiple model parameters) for system with: (a) single  $\theta = [\theta^1]^T$  unknown parameter, (b) double  $\theta = [\theta^1 \ \theta^2]^T$  unknown parameters.

is set to 2 and gains are equal  $\gamma = 20$  and  $\gamma_{mm} = 60$ . The results are presented in Figure 1. The estimated parameter  $\hat{a}, \hat{a}_1, \hat{a}_2$  converges to the plant parameter  $a$ . The behaviour of the system is different in the case of first parameter switch, than in the next switch. As long as parameters  $\hat{a}_1, \hat{a}_2$  converge to the same value, identifier  $e_1$  and  $e_2$  will also do the same.

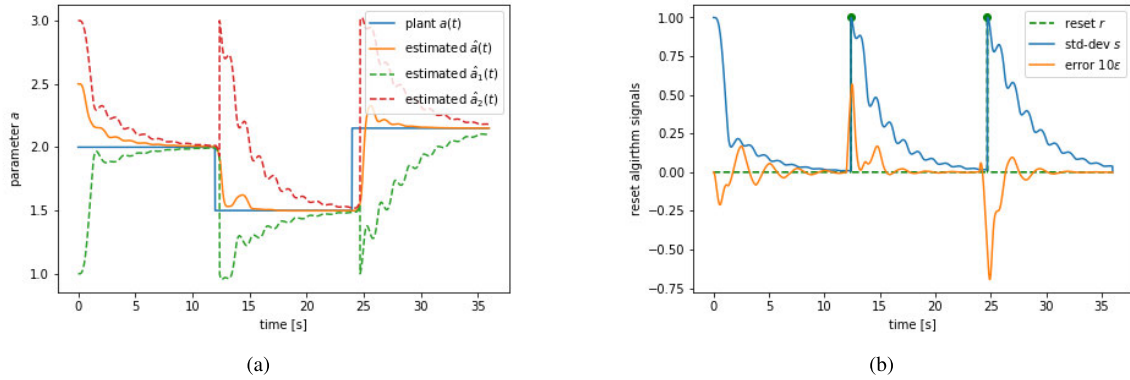


FIGURE 3. Simulation of first order system to present the reset algorithm.

TABLE 1. DEAP actuator nonlinear model parameters.

Parameter	Symbol	Value	Unit
Standard gravity	$g$	9.81	$\frac{m}{s^2}$
Mass	$m$	0.125	$kg$
Vacuum permittivity	$\epsilon_0$	$8.85 \cdot 10^{-12}$	$\frac{F}{m}$
Relative permittivity	$\epsilon_r$	8.73	-
Post-strech tape thickness	$z_0$	200	$\mu m$
Electrode width	$l_0$	65	$mm$
Internal plate radius	$r$	25	$mm$
Damping coefficient	$b$	1.45	$Nm \cdot s$
Coefficient of viscoelastic model	$k_e$	3.11	$MPa$
	$\eta_e$	13.4	$MPa \cdot s$
Ogden model coefficients	$\beta_1$	11.4	$kPa$
	$\beta_2$	50.3	$kPa$
	$\beta_3$	44.1	$kPa$
	$\gamma_1$	-118	$kPa$
	$\gamma_2$	-30.4	$kPa$
	$\gamma_3$	23.3	$kPa$

TABLE 2. The values of high frequency gain, zero and poles for the DEAP actuator transfer function.

Parameter	Symbol	Value	Unit
High frequency gain	$k_p$	$9.3 \times 10^{-8}$	$\frac{m}{V}$
Zero	$z_0$	-0.233	$\frac{1}{s}$
Roots	$s_0$	-0.151	$\frac{1}{s}$
	$s_1$	$-3.2 + 34.3j$	$\frac{1}{s}$
	$s_2$	$-3.2 - 34.3j$	$\frac{1}{s}$

It is clearly visible in Figure 1. This causes, in the case of the second switch, the second layer to be inactive. It is visible that derivative of  $\hat{a}_1$  is almost equal to 0 after the first 10[s]. In such situation, the benefits of multiple model algorithm are not obtained. Hence we propose an algorithm of resetting multiple model structure which allows to cover the presented situation. We would like to reset the values of

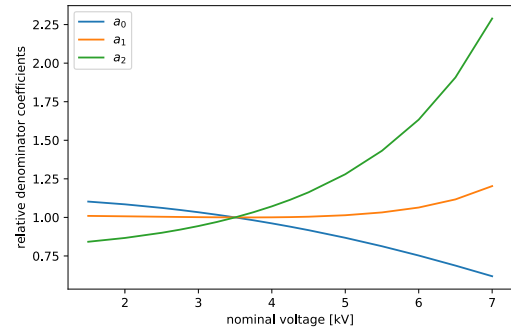


FIGURE 4. Relative denominator coefficients of linear DEAP model for different values of nominal voltage.

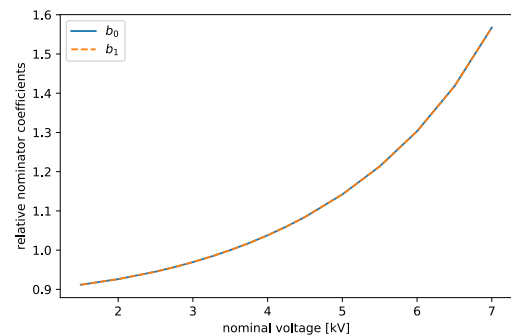
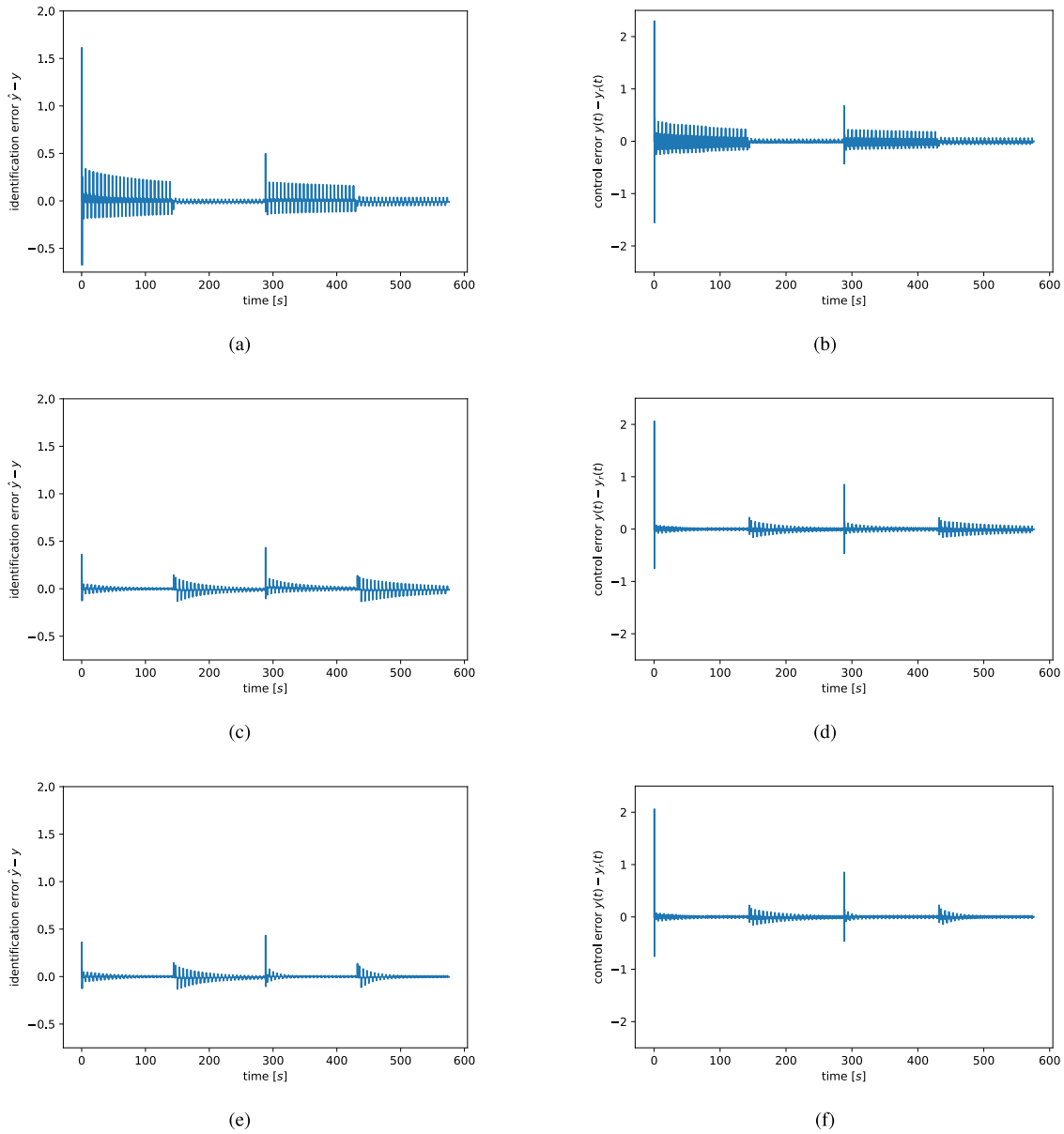


FIGURE 5. Relative nominator coefficients of linear DEAP model for different values of nominal voltage.

TABLE 3. The percentage change of parameters for the DEAP actuator transfer function.

Parameter	Change
$a_0$	38.14[%]
$a_1$	20.4[%]
$a_2$	128.93[%]
$b_0$	56.75[%]
$b_1$	56.75[%]

identifier parameters  $\hat{a}_1, \hat{a}_2$  based on the available signals in the control system.



**FIGURE 6.** Comparison of identification error and tracking error for MRAC (a,b), MRAC-MM (c,d), MRAC-MM-RESET (e,f).

Finally, we describe the main assumptions of resetting algorithm:

- works based on the signals available in the control system,
- notify about the switch of parameters,
- re-initiate the structure of identifiers.

**B. RESETTING ALGORITHM**

The Indirect Model Reference Adaptive Controller with normalized adaptive law assumes only the availability of input and output signals. Therefore, the identifier uses an overparametrized model of plant to express system in input-output representation. The configuration is given by:

$$z = \theta^T \Phi \tag{9}$$

where  $\theta = [\theta^1 \dots \theta^j \dots \theta^{2n}]^T$  is the plant parameter vector with transfer function coefficients,  $z$  is the filtered

output and  $\Phi$  is the filtered input and output (see [16], chapter 2.3 and 6.6). In the case of multiple model extension the adaptive system consists of multiple identifiers and single controller. The number of identifiers depends on the order of system  $n$  and is equal to  $n + 1$ . Hence, the same number of estimated plants is required:

$$\hat{z}_i = \hat{\theta}_i^T \Phi \tag{10}$$

where  $\hat{z}_i$  is the estimated filtered output,  $\hat{\theta}_i$  is the estimated parameters and  $i = 1, \dots, n + 1$ . The vector  $\hat{\theta}_i$  describes a single model of plant and it is calculated by one of available adaptive laws based on gradient, instantaneous cost function or integral cost function [16]. In the case of normalized adaptive laws, the error is expressed as:

$$\epsilon_i = \frac{\hat{z}_i - z}{1 + \Phi^T \Phi} \tag{11}$$

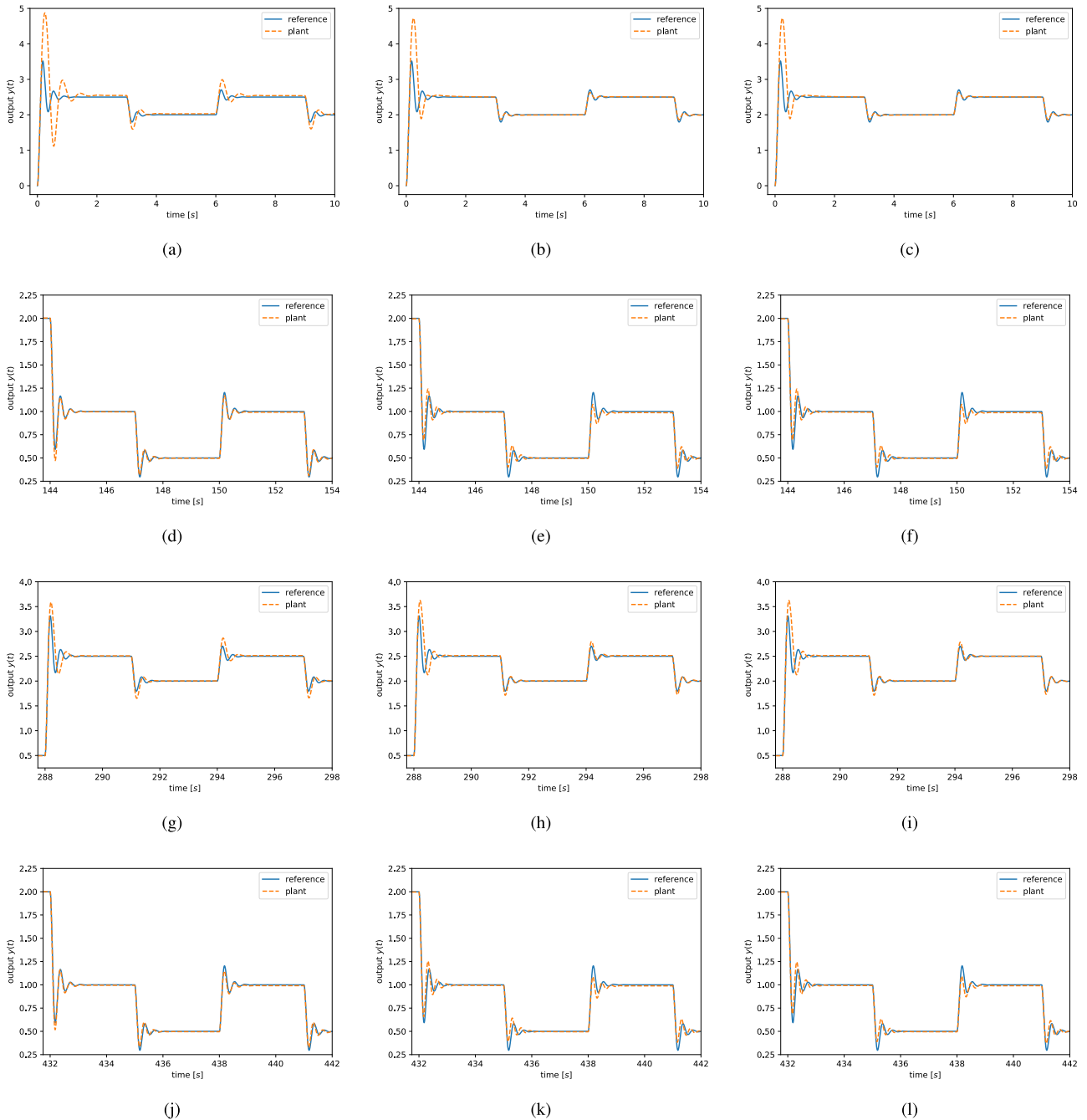


**FIGURE 7. Comparison of output transients zoom for switch at  $t = 0, 144, 288, 432[s]$  for MRAC (a,d,g,j), MRAC-MM (b,e,h,k), MRAC-MM-RESET (c,f,i,l).**

The set of all identifiers creates the first layer of identifier. The goal of the second layer is to calculate an estimation of plant based on the identifiers in the first layer. Based on work [20], the estimated plant parameter  $\hat{\theta}$  is defined as:

$$\hat{\theta} = \sum_{i=1}^{n+1} \hat{\alpha}_i \hat{\theta}_i$$

$$\sum_{i=1}^{n+1} \hat{\alpha}_i = 1 \tag{12}$$

where  $\hat{\alpha}_i$  is the estimated weight of single model. In the second layer the weights  $\hat{\alpha}_i$  are also estimated

by adaptive law given by:

$$\dot{\hat{\alpha}}_i = -\gamma_{mm} (\epsilon_i - \epsilon_{n+1}) \epsilon \tag{13}$$

for  $i = 1, \dots, n$ . The last one is obtained from  $\hat{\alpha}_{n+1} = 1 - \sum_{i=1}^n \hat{\alpha}_i$  and  $\epsilon$  is the error of the second layer:

$$\epsilon = \sum_{i=1}^{n+1} \hat{\alpha}_i \epsilon_i \tag{14}$$

In work [20] it was shown that the existence of adaptation in two layers could provide a better transient performance of an adaptive system with constant parameters.

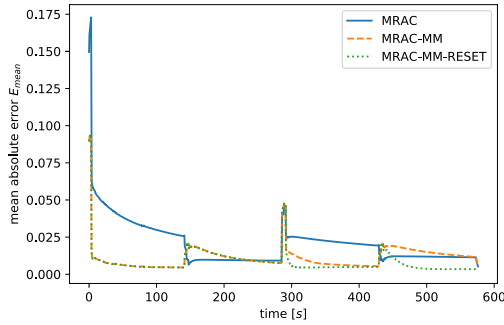


**FIGURE 8.** The function  $E_{mean}$  for MRAC, MRAC-MM and MRAC-MM-RESET.

However, in the case of piecewise constant parameters, as it was shown in the motivation example, the crucial point is to ensure the convex structure of estimated plant parameters  $\hat{\theta}_i$  during the adaption process. This requires a resetting algorithm which will reconstruct the convex hull in the case of parameter value switch. Let us introduce a measure of the deviation of parameters. We define a vector:

$$p_j = \left[ \hat{\theta}_1^j \quad \dots \quad \hat{\theta}_i^j \quad \dots \quad \hat{\theta}_{n+1}^j \right] \quad (15)$$

where  $j = 1, \dots, 2n$ . The standard deviation of  $p_j$  is given by:

$$s_j = \sqrt{\frac{1}{n+1} \sum_{k=1}^{n+1} (p_{kj} - \bar{p}_j)^2} \quad (16)$$

where  $\bar{p}_j$  is the mean of  $p_j$  elements. The standard deviation  $s_j$  describes how much the  $j$  parameter is divergence between multiple models. If the  $j$  parameter is the same for all multiple models, then  $s_j$  is equal 0.

We propose the following reset condition:

$$r = \begin{cases} 1, & \min_{j=1, \dots, 2n} s_j < s_t \wedge |\epsilon| > \epsilon_t \\ 0, & \text{otherwise} \end{cases} \quad (17)$$

where  $s_t$  is threshold for standard deviation and  $\epsilon_t$  is an threshold for identification error. If reset signal  $r$  is 1, the estimated parameters are set to their initial structure. For instance  $r$  is equal 1 at time instant  $t_r$ , then  $\hat{\theta}_i(t_r) = \hat{\theta}_i(0)$ . The expression  $\min_{j=1, \dots, 2n} s_j$  calculates the minimal standard deviation between parameters in multiple models. Hence, the resetting occurs then the identifier have some parameter close each other and an identification error is high. The second condition is introduced to force resetting only if an identification error is high. It is worth mentioning that due to the properties of a standard deviation signal  $s_j$  this resetting condition does not require hysteresis. After the reset, it has some initial value, which should be designed to be higher than  $s_t$ .

In the multiple models algorithm it is possible to choose the structure of parameters. The example of structure for system with order 1 and 2 is presented in Fig. 2. In the moment of switch the initial structure is set again to the

estimated parameters. Hence the value of  $\hat{\theta}$  before the reset differs from value after the reset. This will cause a switch in control  $u$ . From performed simulations, we conclude that such behavior has an adverse effect on control system. However, it is possible to preserve continuity of  $\hat{\theta}$ . Let us denote as  $\hat{\theta}^-$ ,  $\hat{\theta}^+$  the value of estimated parameter before and after switch. The following expression:

$$\hat{\theta}^+ = \sum_{i=1}^{n+1} \hat{\alpha}_i^+ \hat{\theta}_i^0 \quad (18)$$

describes the estimated parameter after switch. In the moment of reset, the coefficients  $\hat{\alpha}_i^+$  are free to choose. Hence, we calculate them to satisfy  $\hat{\theta}^- = \hat{\theta}^+$  from:

$$M \begin{bmatrix} \hat{\alpha}_1^+ \\ \vdots \\ \hat{\alpha}_n^+ \end{bmatrix} = \left[ \theta^- - \theta_{n+1}^0 \right]$$

$$\hat{\alpha}_{n+1}^+ = 1 - \sum_{i=1}^n \hat{\alpha}_i^+$$

$$M = \left[ \theta_1^0 - \theta_{n+1}^0 \quad \dots \quad \theta_n^0 - \theta_{n+1}^0 \right] \quad (19)$$

The matrix  $M$  is invertible as long as  $\theta_i^0$  is chosen by designer and must create a convex hull.

We would like to shortly analyze the algorithm for the motivation example. We set the threshold to  $s_t = 0.05$  and  $\epsilon_t = 0.05$ . The results are visible in Fig. 3. Initial value of  $s_1(0)$  is equal to 1, then it converges to 0. The identification error  $\epsilon$  also converges to 0. The parameter switch (at the time of 12[s]) causes that identification increases and forces the signal reset to 1. This also causes that  $s_1$  come back to 1. It is important to notice that the reset time is not equal to parameter switch time. The identification error signal requires some time to increase, hence in our example the reset is after 0.38[s] and 0.69[s] after the parameter switch.

Another possibility is to use max function in the condition (17). In such case we would choose a parameter with the highest deviation. This means that structure will not be reset until all parameters converge to the same value. However, this is not practical in the case if the converge of parameters differs significantly.

#### IV. SIMULATIONS

In this section we present the simulations of DEAP actuator under the adaptive control. The nonlinear model of the device and its parameters are taken from our previous work [9]. The value of parameters are summarized in Table 1. The linear model  $G_{DEAP}(s)$  is obtained by the linearization of a nonlinear plant in the working point (3) as in our work [32]. The value of  $G_{DEAP}(s)$  is found for the nominal voltage  $u_n = 3.5[kV]$ , which is equal to  $v_n = 12.25[kV^2]$ . The degree of  $Z_p(s)$  and  $R_p(s)$  are 1 and 3 respectively. The transfer function high frequency gain, zeros and poles are presented in Table 2.

The parameters of  $G_{DEAP}(s)$  depend on the nominal working point. To find how much the parameter vary for

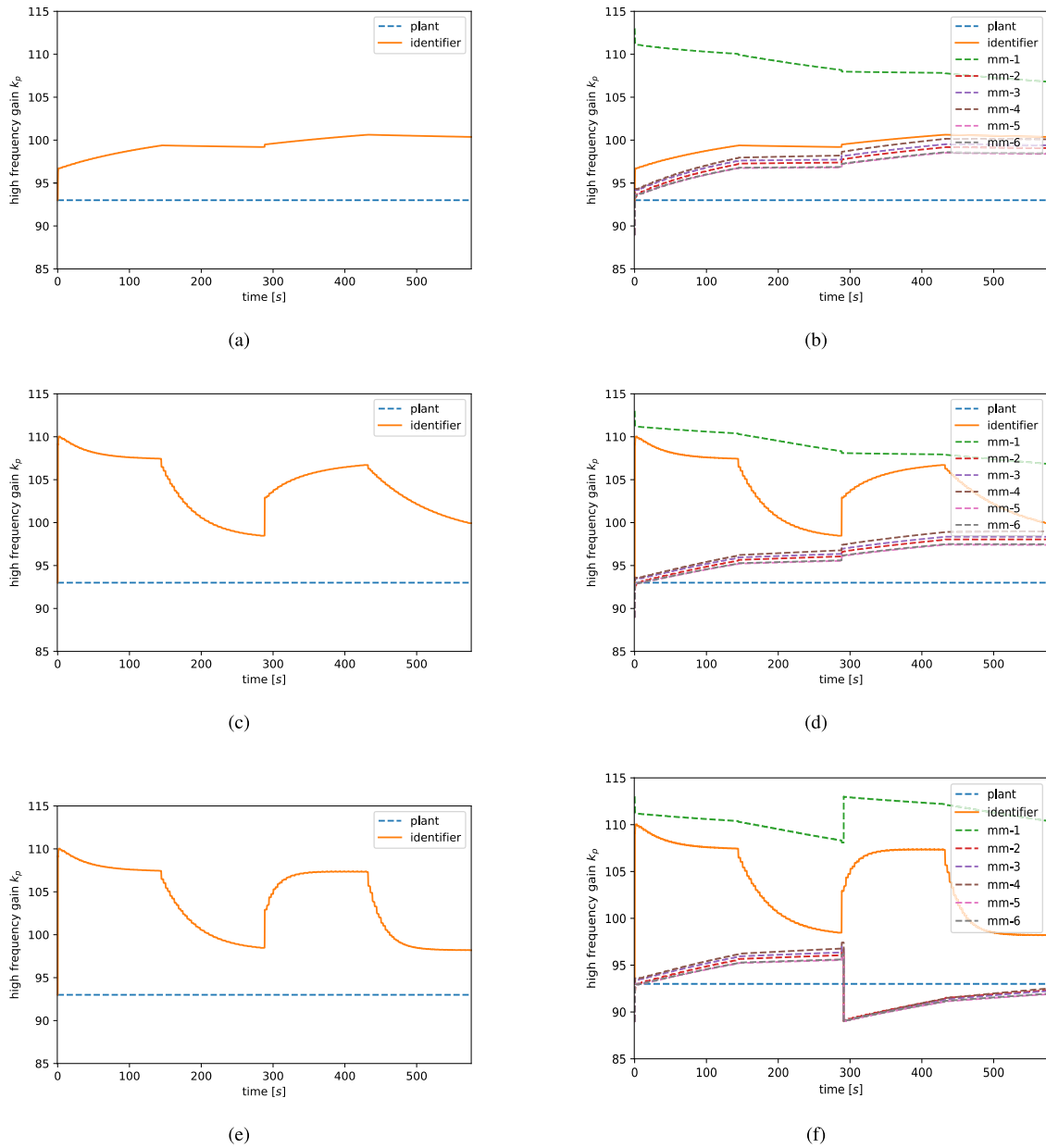


FIGURE 9. Comparison parameter transients for MRAC (a,b), MRAC-MM (c,d), MRAC-MM-RESET (e,f).

different working points, we calculate the coefficients of polynomials  $k_p Z_p(s) = b_1 s + b_0$  and  $R_p(s) = s^3 + a_2 s^2 + a_1 s + a_0$ . The value of coefficients was found by a linearization of a nonlinear plant for a range  $1.5 - 7[kV]$ . Their relative values are presented in Fig. 4 and 5. The percentage change of parameters for the DEAP actuator transfer function is presented in Table 3.

A. ADAPTIVE CONTROL

In this section we present the adaptive control designed to DEAP actuator. We assume that the device is working in some nominal point for a period of time, and due to reference command or external signal (like load torque) is changing the working point. As stated in the previous part, the coefficients

of the linear model are varying hence the adaptation is required to find new parameter values. In the case of MRAC the reference model is chosen with roots  $s_{1m} = -5 + j17.5$  and  $s_{2m} = -5 - j17.5$  and static gain equal to 1. The overparametrized plant model (10) is constructed by applying filter with roots  $\lambda = -10$ . The multiple models structure is applied in the identifier. Therefore, the number of identifiers is equal to 4 (the system has order 3). In the first layer the adaptation is performed by least square algorithm with gain  $P_0 = 100$  and  $P_0 = 500$ . In the second layer the adaption gain  $g_{mm}$  has value 5. The reset algorithm thresholds (17) are set as follows:  $s_t = 2.0$ ,  $\epsilon_t = 0.05$ . The Model Reference Controller is built based on the estimated parameters from the identifier.



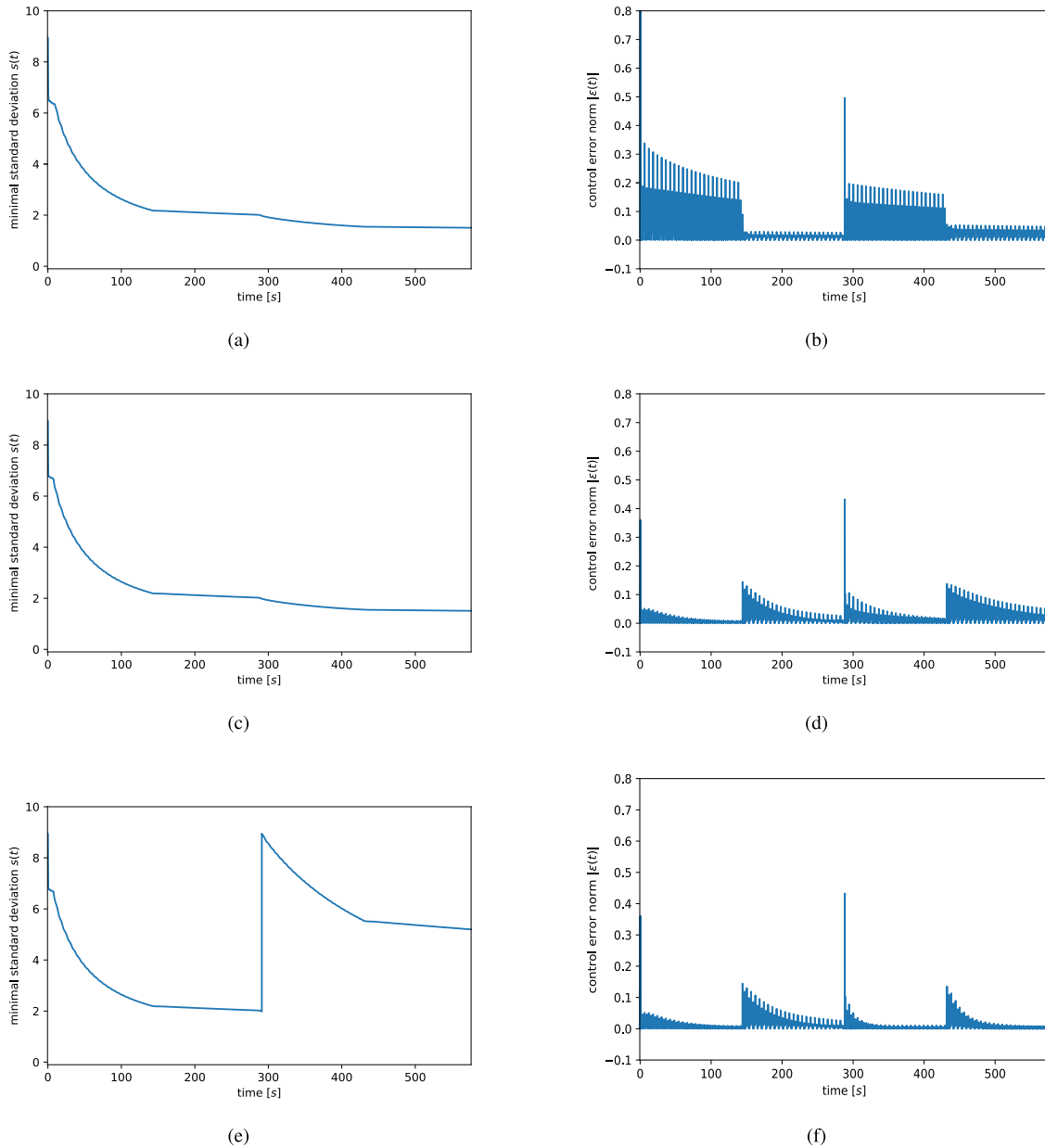


**FIGURE 10.** Comparison reset algorithm signals for MRAC (a,b), MRAC-MM (c,d), MRAC-MM-RESET (e,f).

To perform the analysis of adaptive control systems, the three variants of controller are studied. The first is denoted as MRAC (Model Reference Adaptive Control - without the multiple models and without resetting), the second as MM-MRAC (MRAC with multiple models), and the third as MM-RESET-MRAC (MRAC with multiple models and resetting algorithm). The performance indexes was calculated for the control system running the following trajectory:

$$y_r(t) = 1.5 + 0.75 \text{sign}(\sin(\frac{2\pi}{T_1}t)) + 0.25 \text{sign}(\sin(\frac{2\pi}{T_2}t)) \quad (20)$$

with  $T_1 = 288[s]$  and  $T_2 = 6[s]$ . This means that the parameter switch due to change of nominal point is after each 144[s]. The simulations are done for two levels of gains:  $P_0 = 100$  and  $P_0 = 500$ . To limit the space the plots

are shown for  $P_0 = 100$ . The identification and control error are visible in Fig. 6 and the zoom of the output is shown in Fig. 7. It is visible at time 144[s], 288[s], ... the change of reference signal amplitude causes the requirement of adaptation. To simplify the comparison of the algorithms, the auxiliary function is introduced for the control error:

$$E_{mean}(t) = \frac{1}{T_2} \int_{t-\frac{T_2}{2}}^{t+\frac{T_2}{2}} |\bar{e}(\tau)| d\tau$$

$$\bar{e}(t) = \begin{cases} e(t), & 0 \leq t \leq T_f \\ 0, & \text{otherwise} \end{cases} \quad (21)$$

where  $T_f$  is the final time of the simulations. The function  $E_{mean}(t)$  calculates the mean absolute of the control error for the time  $T_2$ . The results for the three algorithms are presented

TABLE 4. Performance indexes for  $P_0 = 100$ .

Method	$J_{ISE}$	$J_{IAE}$	$J_{ITAE}$
MRAC	2.0719	12.3517	2640.3679
MM-MRAC	0.9449	6.6778	1952.5798
MM-RESET-MRAC	0.8702	4.9648	1150.3923

TABLE 5. Performance indexes for  $P_0 = 500$ .

Method	$J_{ISE}$	$J_{IAE}$	$J_{ITAE}$
MRAC	1.2028	8.4458	2218.4979
MM-MRAC	0.8978	7.2396	2175.3646
MM-RESET-MRAC	0.8259	3.9251	948.2759

in Fig. 8. The process of adaption is shown in Fig. 9 for single parameter  $k_p$ . In the Fig. 10 the reset algorithm signal is shown. The structure is reset for the switch at the time 288[s] with small delay. The performance indexes are shown in Table 4 and 5 for gain  $P_0 = 100$  and  $P_0 = 500$  respectively. It is visible that for all indexes the control method MM-RESET-MRAC provides the transient improvement.

## V. CONCLUSIONS

In this work, the indirect adaptive controller is designed for a DEAP actuator. The recent technique multiple models with the second level adaption is applied to obtain the transient improvement. Due to the parameter convergence for long time operation, the resetting algorithm was proposed. Additionally, the new signals, which describes the behavior of multiple models was defined. This approach allows to reset the multiple model structure, hence the long time operation under varying condition is possible. The quantitative improvement is shown based on performance indexes. In this work the main features are: a new algorithm to reset multiple models structure, the analysis of multiple models adaptation for long time operation and adaptive control scheme for a DEAP actuator. In the future works, the extension to nonlinear adaptive control methods can be applied [19], [34].

## REFERENCES

- [1] Y. Bar-Cohen, *Electroactive Polymer (EAP) Actuators as Artificial Muscles: Reality, Potential, and Challenges*. Bellingham, WA, USA: SPIE, 2001.
- [2] C. Cao, X. Gao, and A. T. Conn, "A magnetically coupled dielectric elastomer pump for soft robotics," *Adv. Mater. Technol.*, vol. 4, no. 8, Aug. 2019, Art. no. 1900128.
- [3] I. A. Anderson, T. A. Gisby, T. G. McKay, B. M. O'Brien, and E. P. Calius, "Multi-functional dielectric elastomer artificial muscles for soft and smart machines," *J. Appl. Phys.*, vol. 112, no. 4, Aug. 2012, Art. no. 041101.
- [4] K. J. Kim and S. Tadokoro, *Electroactive Polymers for Robotic Applications: Artificial Muscles and Sensors*. London, U.K.: Springer-Verlag, 2007.
- [5] S. Rosset and H. R. Shea, "Small, fast, and tough: Shrinking down integrated elastomer transducers," *Appl. Phys. Rev.*, vol. 3, no. 3, Sep. 2016, Art. no. 031105.
- [6] R. Sarban, B. Lassen, and M. Willatzen, "Dynamic electromechanical modeling of dielectric elastomer actuators with metallic electrodes," *IEEE/ASME Trans. Mechatronics*, vol. 17, no. 5, pp. 960–967, Oct. 2012.
- [7] G. Rizzello, M. Hodgins, D. Naso, A. York, and S. Seelecke, "Modeling of the effects of the electrical dynamics on the electromechanical response of a DEAP circular actuator with a mass–spring load," *Smart Mater. Struct.*, vol. 24, no. 9, Aug. 2015, Art. no. 094003.
- [8] G. Rizzello, D. Naso, B. Turchiano, and S. Seelecke, "Robust position control of dielectric elastomer actuators based on LMI optimization," *IEEE Trans. Control Syst. Technol.*, vol. 24, no. 6, pp. 1909–1921, Nov. 2016.
- [9] J. Bernat and J. Kolota, "Adaptive observer for state and load force estimation for dielectric electro-active polymer actuator," in *Proc. 11th IFAC Symp. Nonlinear Control Syst.*, Sep. 2019, pp. 448–453.
- [10] M. Zhang, X. Cao, X. Chen, Z. Zhang, Z. Chen, and T. Li, "Model-based nonlinear control of the dielectric elastomer actuator with high robustness and precision," *J. Appl. Mech.*, vol. 86, no. 12, Dec. 2019.
- [11] J. Zou and G. Gu, "Feedforward control of the rate-dependent viscoelastic hysteresis nonlinearity in dielectric elastomer actuators," *IEEE Robot. Autom. Lett.*, vol. 4, no. 3, pp. 2340–2347, Jul. 2019.
- [12] T. Hoffstadt and J. Maas, "Adaptive sliding-mode position control for dielectric elastomer actuators," *IEEE/ASME Trans. Mechatronics*, vol. 22, no. 5, pp. 2241–2251, Oct. 2017.
- [13] A. Poulin and S. Rosset, "An open-loop control scheme to increase the speed and reduce the viscoelastic drift of dielectric elastomer actuators," *Extreme Mech. Lett.*, vol. 27, pp. 20–26, Feb. 2019.
- [14] L. Li, J. Li, L. Qin, J. Cao, M. S. Kankanhalli, and J. Zhu, "Deep reinforcement learning in soft viscoelastic actuator of dielectric elastomer," *IEEE Robot. Autom. Lett.*, vol. 4, no. 2, pp. 2094–2100, Apr. 2019.
- [15] P. R. Massenio, G. Rizzello, and D. Naso, "Fuzzy adaptive dynamic programming minimum energy control of dielectric elastomer actuators," in *Proc. IEEE Int. Conf. Fuzzy Syst. (FUZZ-IEEE)*, Jun. 2019, pp. 1–6.
- [16] P. Ioannou, *Robust Adaptive Control*. Los Angeles, Ca, USA: Univ. of Southern California, 2003.
- [17] S. Haykin, *Adaptive Filter Theory*. Upper Saddle River, NJ, USA: Prentice-Hall, 2001.
- [18] K. S. Narendra and Z. Han, "The changing face of adaptive control: The use of multiple models," *Annu. Rev. Control*, vol. 35, no. 1, pp. 1–12, Apr. 2011.
- [19] K. Sun, L. Liu, J. Qiu, and G. Feng, "Fuzzy adaptive finite-time fault-tolerant control for strict-feedback nonlinear systems," *IEEE Trans. Fuzzy Syst.*, early access, Jan. 13, 2020, doi: 10.1109/TFUZZ.2020.2965890.
- [20] Z. Han and K. S. Narendra, "New concepts in adaptive control using multiple models," *IEEE Trans. Autom. Control*, vol. 57, no. 1, pp. 78–89, Jan. 2012.
- [21] W. Zhang and L. Zhao, "Survey and tutorial on multiple model methodologies in modelling, identification and control," *Int. J. Model., Identificat. Control*, vol. 32, no. 1, pp. 1–9, 2019.
- [22] K. S. Narendra and Z. Han, "Adaptive control using collective information obtained from multiple models," in *Proc. 18th IFAC World Congr.*, Aug. 2011, pp. 1–6.
- [23] V. Pandey, I. Kar, and C. Mahanta, "Multiple model adaptive control using second level adaptation for a class of nonlinear systems with linear parameterizations," *Int. J. Dyn. Control*, vol. 6, no. 3, pp. 1319–1334, Sep. 2018.
- [24] J. Bernat, "Multiple model adaptive control applied to fractional order systems," in *Proc. 22nd Int. Conf. Methods Models Autom. Robot. (MMAR)*, Aug. 2017, pp. 488–493.
- [25] J. Bernat and S. Stepien, "Multi-modelling as new estimation schema for high-gain observers," *Int. J. Control*, vol. 88, no. 6, pp. 1209–1222, Jun. 2015.
- [26] J. Bernat, J. Kolota, P. Superczynska, and S. Stepien, "Multi-layer observer as new structure for state estimation in linear systems," *Arch. Electr. Eng.*, vol. 66, no. 3, pp. 507–521, Sep. 2017.
- [27] K. Narendra, *Hierarchical Adaptive Control of Rapidly Time-Varying Systems Using Multiple Models*. New Haven, CT, USA: Yale Univ., 2016.
- [28] J. Skach, B. Kiumarsi, F. L. Lewis, and O. Straka, "Actor-critic off-policy learning for optimal control of multiple-model discrete-time systems," *IEEE Trans. Cybern.*, vol. 48, no. 1, pp. 29–40, Jan. 2018.
- [29] J. Bernat and J. Kolota, "Integral multiple models online identifier applied to ionic polymer–metal composite actuator," *J. Intell. Mater. Syst. Struct.*, vol. 29, no. 14, pp. 2863–2873, Aug. 2018.
- [30] Q. Yin, M. Wang, and W. Zhao, "Adaptive switching control based on limited multiple models," *Int. J. Adapt. Control Signal Process.*, vol. 33, no. 6, pp. 913–925, 2019.
- [31] K. S. Narendra and K. Esfandiari, "Adaptive identification and control of linear periodic systems using second-level adaptation," *Int. J. Adapt. Control Signal Process.*, vol. 33, no. 6, pp. 956–971, Jun. 2019.

- [32] J. Bernat and L. Kolota, "Adaptive controller with output feedback for dielectric electro-active polymer actuator," in *Proc. 12th Int. Workshop Robot Motion Control (RoMoCo)*, Jul. 2019, pp. 247–251.
- [33] G. Rizzello, D. Naso, A. York, and S. Seelecke, "Modeling, identification, and control of a dielectric electro-active polymer positioning system," *IEEE Trans. Control Syst. Technol.*, vol. 23, no. 2, pp. 632–643, Mar. 2015.
- [34] M. Krstic, I. Kanellakopoulos, and P. V. Kokotovic, *Nonlinear and Adaptive Control Design*. New York, NY, USA: Wiley, 1995.



**JAKUB BERNAT** (Member, IEEE) received the M.Sc. and Ph.D. degrees from the Poznan University of Technology, in 2007 and 2011, respectively. He is currently a Postdoctoral Fellow of the Faculty of Computer Science, Poznan University of Technology. His main research areas are control theory, adaptive systems, robust control, and state estimation. He is currently working on the control of electroactive polymers and nonlinear adaptive control.



**JAKUB KOŁOTA** received the M.Sc. and Ph.D. degrees from the Poznan University of Technology, Poland, in 2005 and 2009, respectively. In the Ph.D. degree thesis, he described a complex simulation of a stepper motor, represented in 3D space with distributed parameters. He is currently a Research Scientist with the Faculty of Control, Robotics, and Electrical Engineering, Poznan University of Technology. His research interests include nonlinear electromagnetic field analysis and synthesis, PLC controllers, cloud computing, and control theory in smart materials. He is currently working on electroactive polymers such as the IPMC and DEAP.



**DAMIAN CIEŚLAK** received the B.Sc. degree from the Poznan University of Technology, in 2018, and the master's degree in automation and robotics from the Faculty of Computer Science, Poznan University of Technology, in 2019. He is currently working on the control of electroactive polymers and adaptive control.

...